International Current Journal of Engineering and Science (ICJES)
Volume 5, Issue 5, pp 9-17, May-2026
ISSN (Online): 2583-7257
Article DOI: https://doi.org/10.47001/ICJES/2026.505002

CFD-DPM Based Prediction of Erosion Rate in Elbow Pipe under Seawater Flow Conditions

[1]*Muchammad, [2]Budi Setiyana, [3]Galang Hardhian Prasetyo

[1,2,3]Mechanical Engineering Department, Faculty of Engineering, Diponegoro University, Jl. Prof. H. Soedarto, SH, Tembalang-Semarang 50275, Indonesia
*Corresponding Author's E-mail: muchammad5373@gmail.com

Abstract **- Erosion due to the interaction of solid particles in fluid flow is one of the main causes of material degradation in piping systems, especially at the elbow sections where the flow direction changes. This phenomenon can reduce the reliability and service life of the pipe due to particle impacts concentrated in certain areas. This study aims to analyze the influence of variations in particle size, particle concentration, flow velocity, and elbow geometry on the erosion rate in piping systems. The method used is Computational Fluid Dynamics (CFD) simulation using ANSYS Fluent with a two-phase flow approach (continuous phase and discrete phase) and the Oka erosion model. The parameter variations include particle sizes of 150–350 µm, particle concentrations of 100–300 ppm, flow velocities of 5.5–7.4 m/s, and four types of elbow geometries. The simulation results show that particle size and concentration have the most significant impact on the increase in erosion rate, with erosion values increasing from 7.24 × 10^{-8} to 2.37 × 10^{-7} kg/m²s and from 1.36 × 10^{-7} to 4.09 × 10^{-7} kg/m²s. Meanwhile, the influence of flow velocity is relatively smaller within the range studied. Geometric variations show that single and multi miter bends increase the erosion rate, while reducer elbows decrease it. The maximum erosion distribution occurs at the outer radius elbow due to the particle inertia effect. The results of this study are expected to serve as a basis for optimizing the design and operation of piping systems against erosion.**

Keywords: CFD, pipe erosion, particle size, particle concentration, flow velocity, elbow geometry, Oka erosion model.

I. INTRODUCTION

Piping systems serve as the backbone of fluid transport across numerous industrial sectors, from oil and gas facilities to marine engineering and thermal power plants. Among all piping components, elbows are consistently identified as the most erosion-prone sections, as the abrupt change in flow direction forces solid particles to deviate from the fluid streamline due to inertia, causing them to impinge directly on the outer wall and accelerate material loss. This phenomenon, known as solid particle erosion (SPE), poses a persistent threat to the structural integrity and service life of piping systems in continuous operation (Mahmoudi and Siri, 2025).

The severity of erosion in pipe elbows is shaped by several interacting factors, including particle size, concentration, flow velocity, and elbow geometry, each of which governs the energy transferred during particle-wall impact. In liquid-solid two-phase flow conditions such as those found in seawater cooling systems, this interaction becomes particularly complex, as the density and viscosity of the carrier fluid significantly alter particle trajectories compared to gas-solid systems. Studies addressing erosion specifically under liquid-solid flow conditions remain relatively scarce, and predictive accuracy across different elbow configurations still requires further validation (Yasser et al., 2025; Rahman et al., 2025).

The CFD-DPM approach has emerged as a reliable and cost-effective alternative to experimental erosion testing. Veiskarami and Saidi (2024) demonstrated through CFD-DPM simulation that alternative elbow geometries could reduce maximum erosion by 22.5% to 39.6% compared to a standard 90° elbow, while Yasser et al. (2025) showed that particle shape plays a critical role in determining erosion intensity and spatial distribution. These findings confirm that both geometric and operational parameters must be systematically evaluated to generate erosion predictions relevant to real engineering applications.

Despite this growing body of knowledge, most existing CFD erosion studies focus on gas-solid flow in industrial pipelines, and very few address the marine seawater cooling context specifically. Seawater piping components in vessels are inherently exposed to a dual degradation mechanism: the corrosive nature of seawater and the continuous mechanical impingement of fine sediment particles entrained in the flow, particularly when vessels operate in shallow coastal waters or

International Current Journal of Engineering and Science (ICJES)
Volume 5, Issue 5, pp 9-17, May-2026
ISSN (Online): 2583-7257
Article DOI: https://doi.org/10.47001/ICJES/2026.505002

port areas where sediment resuspension is common (Sridhar and Balasubramanian, 2022; Davidson et al., 2021).

This study addresses that gap by applying the CFD-DPM method with the Oka erosion model and RSM turbulence closure to predict erosion rates in a 90° long-radius elbow under seawater flow conditions. Particle size (150 to 350 µm), concentration (100 to 300 ppm), flow velocity (5.5 to 7.4 m/s), and four elbow geometry variants are systematically investigated, along with post-simulation estimations of wall thinning rate and remaining service life based on ASME B31.3. The physical reference is a seawater supply elbow pipe from a marine auxiliary engine cooling system, selected based on significant wall thinning and erosion-corrosion damage identified during routine inspection.

II. RESEARCH OBJECT

2.1 Seawater Supply Elbow Pipe

The research object in this study is a 90° long-radius elbow pipe serving as part of the seawater supply line in an auxiliary engine cooling system aboard a passenger vessel. The elbow pipe has an outside diameter of 89.1 mm, a wall thickness of 7.6 mm, and is fabricated from carbon steel material (JIS G3454, equivalent to ASTM A53 Grade A). This component functions as a flow-directing element that channels seawater from the sea chest intake through the cooling circuit to dissipate heat generated by the auxiliary engine during vessel operation. The elbow was selected as the research object following the identification of significant wall thinning and surface deterioration at the outer radius section during a routine inspection, a condition consistent with erosion-corrosion damage typical of seawater piping systems in marine applications. The schematic of the elbow pipe geometry used in this study can be seen in Figure 1.

Figure 1: Seawater Supply Elbow Pipe

The detailed geometric specifications of the elbow pipe model employed in the simulation are listed in Table 1.

Table 1: Detail Geometric of Elbow Pipe

Parameter	Value
Outside Diameter	89,1 mm
Inside Diameter	73,9 mm
Thickness	7,6 mm
Horizontal Length	210 mm
Verical Length	1750 mm
Elbow Type	90° *Long Radius*
Elbow Radius	114°

2.1 Governing Equation

2.2.1 Fluid Flow Equations

The fluid flow behavior in this study is governed by the conservation principles of mass and momentum, which are expressed through the continuity equation and the Reynolds-Averaged Navier-Stokes (RANS) equations. The continuity equation ensures that mass is conserved throughout the flow domain. In simple terms, whatever seawater enters the elbow pipe must also exit it without any loss. The continuity equation ensures that mass is conserved throughout the flow domain, whatever seawater enters the elbow pipe must also exit without any loss. The RANS momentum equation describes how the fluid accelerates and decelerates as it navigates the elbow geometry, accounting for the effects of pressure gradients, viscous stresses, and turbulent fluctuations (Martin et al., 2014). These two equations are expressed as:

$$\frac{\partial p}{\partial t} + \nabla.(\rho\vec{u}) = 0 \quad (1)$$

$$\frac{\partial(\,(\rho\vec{u})}{\partial t} + \nabla.(\rho\vec{u}\vec{u}) = -\nabla p + \nabla\cdot(\mu eff\nabla u) \quad (2)$$

where $\rho$is the fluid density, $\vec{u}$is the velocity vector, p is the static pressure, and μ_{eff} is the effective dynamic viscosity that incorporates both molecular and turbulent contributions.

2.2.2 Turbulence Model

Accurate turbulent flow prediction requires selecting a model that is appropriate for the specific flow geometry under investigation. The RANS-based turbulence models are broadly categorized by the number of transport equations they solve: the one-equation Spalart-Allmaras model solves for turbulent viscosity directly, while two-equation models such as k-ε and k-ω solve separately for turbulent kinetic energy and its dissipation or specific dissipation rate. However, two-equation models are known to perform less accurately in flows involving strong streamline curvature, system rotation, and secondary flow structures, conditions that are inherently

International Current Journal of Engineering and Science (ICJES)
Volume 5, Issue 5, pp 9-17, May-2026
ISSN (Online): 2583-7257
Article DOI: https://doi.org/10.47001/ICJES/2026.505002

present inside elbow pipe geometries (Veiskarami and Saidi, 2024; Yasser et al., 2025).

To address this limitation, the present study employs the Reynolds Stress Model (RSM), which solves seven additional transport equations in three-dimensional flow, six for the individual Reynolds stress components and one for the dissipation rate. This approach avoids the isotropic eddy viscosity assumption and therefore captures anisotropic turbulence behavior more accurately, particularly in regions of swirling flow, strong eddy currents, and curved streamlines that characterize 90° elbow flows. The governing transport equation of the RSM is expressed as:

$$\frac{\partial}{\partial t}(\rho\overline{ui'\,uj'}) + \frac{\partial}{\partial xk}(\rho u_k\overline{ui'\,uj'}) = Pij + \Pi ij - \varepsilon ij + Di \quad (3)$$

where P_{ij} is the stress production term, Π_{ij} is the pressure-strain correlation, ε_{ij} is the dissipation tensor, and D_{ij} represents turbulent and molecular diffusion. Together, these terms describe how turbulent energy is generated, redistributed, and eventually dissipated within the curved flow domain.

2.2.3 Discrete Phase Model (DPM)

To simulate the motion of sand particles transported by seawater, this study employs the Discrete Phase Model (DPM) within anEulerian-Lagrangian framework. The DPM is a Eulerian-Lagrangian approach to tracking individual particles, which enables a detailed description of the motion processes of particles including collision and rotation behavior (Dou et al., 2023). In this approach, the seawater is treated as a continuous phase solved via the RANS equations, while each sand particle is individually tracked by integrating Newton's second law of motion along its trajectory through the flow domain. The particle motion is mainly determined by the drag force and gravity force, both of which are essential for producing accurate particle tracking results in curved pipe geometries (Arabnejad et al., 2025**)**. At the elbow section, the inertia of each particle resists the sudden change in flow direction, causing it to deviate from the fluid streamlines and strike the outer pipe wall, the fundamental physical mechanism responsible for erosion. The particle equation of motion is expressed as:

$$\frac{d\vec{u}_p}{dt} = \vec{F}_D + \vec{F}_P + \vec{F}_G + \vec{F}_{VM} + \vec{F} \quad (4)$$

where $\vec{u}_p$ is the particle velocity (m/s), ρ_p is the particle density (kg/m³), $\vec{g}$ is gravitational acceleration (m/s²), and F_D is the drag force coefficient per unit mass, defined as:

$$\overrightarrow{F_D} = \frac{18\mu_f}{\rho_p\, d_p^2}\frac{C_D Re_p}{24}\left(\overrightarrow{\mu_f} - \overrightarrow{\mu_p}\right) \quad (5)$$

Here, d_p is the particle diameter (m), C_D is the drag coefficient, and Re_p is the particle Reynolds number. This formulation ensures that the trajectory of each particle is physically consistent with the fluid forces it experiences throughout its journey through the elbow.

2.2.4 Oka Erosion Model

Once the particle trajectories and impact conditions are established through the DPM, the resulting erosion rate on the pipe wall is calculated using the Oka erosion model. This model was specifically developed and validated for liquid-solid two-phase flow conditions, making it more appropriate for the seawater environment in this study compared to erosion models originally derived for gas-solid systems. The Oka model computes the erosion rate as a function of particle impact velocity, impact angle, and particle size, capturing the physical reality that faster and larger particles striking the wall at more aggressive angles will cause proportionally greater material loss. The erosion rate is expressed as:

$$E_R = E_{90} \cdot f(\alpha) \cdot \left(\frac{V_p}{V_{ref}}\right)^{k_2} \cdot \left(\frac{d_p}{d_{ref}}\right)^{k_3} \quad (6)$$

where E_{90} is the reference erosion rate at a 90° impact angle (kg/m²), $f(\alpha)$ is the impact angle function, V_p is the particle impact velocity (m/s), V_{ref} is the reference velocity (m/s), d_p is the particle diameter (m), d_{ref} is the reference particle diameter (m), and k_2, k_3 are empirical constants dependent on the target material properties. The angle function $f(\alpha)$ is defined as:

$$f(\alpha) = (\sin\alpha)^{n_1} \cdot (1 + H_v(1 - \sin\alpha))^{n_2} \quad (7)$$

where α is the particle impact angle, H_v is the Vickers hardness of the wall material, and n_1, n_2 are material-dependent exponents. This formulation reflects the well-established physical understanding that both the speed and the angle at which a particle strikes a surface are critical determinants of the resulting wear rate (Oka & Yoshida, 2005).

III. METHODS

3.1 Geometry & Mesh

The three-dimensional geometry of the elbow pipe in this study was constructed using ANSYS Design Modeler based on the actual dimensional specifications of the seawater supply elbow pipe retrieved from the vessel's piping documentation during inspection. The pipe geometry adopts

International Current Journal of Engineering and Science (ICJES)
Volume 5, Issue 5, pp 9-17, May-2026
ISSN (Online): 2583-7257
Article DOI: https://doi.org/10.47001/ICJES/2026.505002

an inside diameter of 73.9 mm, an outside diameter of 89.1 mm, a wall thickness of 7.6 mm, and an elbow bend radius of 114 mm. The straight pipe sections extend 210 mm on the horizontal leg and 1.750 mm on the vertical leg, providing sufficient hydraulic development length upstream of the elbow to ensure a fully developed turbulent velocity profile at the inlet. The pipe material is Carbon Steel STPG 370-E (equivalent to ASTM A53 Grade A, JIS G3454), with a density of 7.850 kg/m³, a tensile strength of 370 MPa, and a yield strength of 215 MPa. The seawater continuous phase is assigned a density of 1,023 kg/m³ and a dynamic viscosity of 9.38×10^{-4} Pa·s, while the discrete sand particles (SiO_2) are assigned a density of 2.650 kg/m³. To evaluate the influence of elbow configuration on erosion behavior, four geometric variants were modeled and compared in this study, as illustrated in Figure 2: (1) standard 90° long-radius elbow as the baseline geometry, (2) single-piece miter bend and (3) multi-piece miter bend representing abrupt flow deflection with no curvature radius, and (4) reducer elbow incorporating a gradual cross-sectional area reduction along the bend, all can be seen in Figure 2.

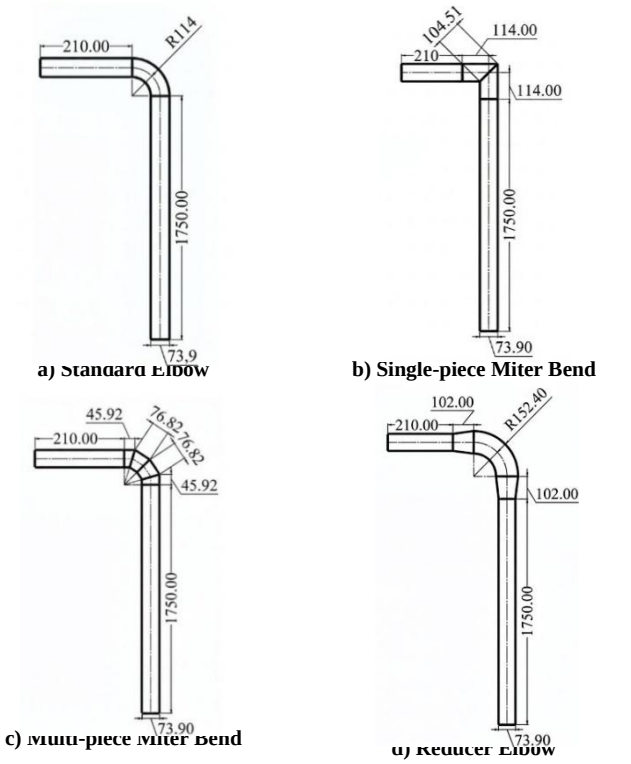

Figure 2: Variations in Elbow Geometry

The computational mesh for all geometry variants was generated within the ANSYS Meshing environment using a structured meshing strategy. To build the mesh, two Edge Sizing operations were applied to the radial and circumferential edges of the pipe cross-section, each configured with a Number of Divisions. The Multizone method was then assigned to the entire pipe body, which automatically decomposes the geometry into structured hexahedral elements, a topology well-suited for internal pipe flow where the flow direction is clearly defined. To capture the steep velocity gradients near the pipe wall, where particle-wall interactions are most concentrated, a bias factor of 3 was applied to progressively refine the mesh toward the wall surface. The resulting mesh configuration provides sufficient spatial resolution to accurately resolve both the bulk turbulent flow behavior and the near-wall erosion dynamics throughout the elbow geometry. The meshing results can be seen below in Figure 3.

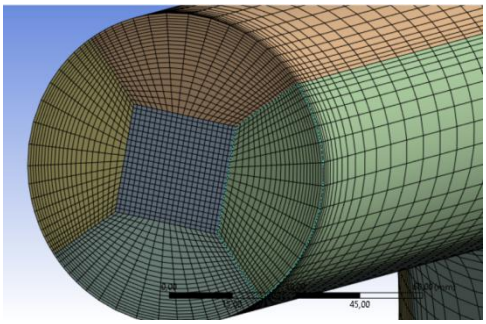

Figure 3: Meshing Results

3.2 Boundary Conditions

The boundary conditions in this simulation are divided into two categories corresponding to the two-phase flow framework, the continuous phase and the discrete phase.

For the continuous phase, seawater enters the domain from the bottom of the vertical pipe leg through a velocity inlet, with inlet velocities varied across five values ranging 5.5, to 7.4 m/s, representing the operational range of the seawater supply pump. The flow then travels upward through the 1,750 mm vertical leg, navigates the 90° elbow with a bend radius of 114 mm, continues along the 210 mm horizontal leg, and exits through a pressure outlet fixed at 0 Pa gauge pressure. All pipe wall surfaces are treated with a no-slip condition, enforcing zero fluid velocity at the wall boundary. Gravitational acceleration of $g = 9.81$ m/s² is applied in the vertically downward direction, consistent with the physical pipe orientation.

For the discrete phase, sand particles (SiO_2) are injected at the inlet surface with velocities equal to the local fluid velocity at each respective simulation case. Particle concentration is varied between 100 and 300 ppm, and particle diameters range from 150 to 350 µm. Upon reaching the pipe wall, particles are assigned a Reflect condition, allowing them to rebound elastically and physically consistent with the hard

International Current Journal of Engineering and Science (ICJES)
Volume 5, Issue 5, pp 9-17, May-2026
ISSN (Online): 2583-7257
Article DOI: https://doi.org/10.47001/ICJES/2026.505002

particle-steel wall interaction. At both the inlet and outlet boundaries, an Escape condition is applied, whereby particles exiting these boundaries are removed from the tracking domain.

3.3 Post Simulation

The erosion rate values obtained from the CFD-DPM simulation represent the contribution of mechanical particle impingement alone. In practice, however, the actual material degradation in the seawater supply pipe is driven by a combined erosion-corrosion mechanism. The lifetime estimations presented in this study therefore represent an upper boundary of the actual service life, as the corrosion contribution is not accounted for in the numerical model, but represents as a corrosion allowance.

The wall thinning rate is calculated by dividing the maximum erosion rate obtained from simulation by the pipe material density (Carbon Steel STPG 370-E, ρ= 7,850 kg/m³), yielding a thinning rate in units of m/s. This value is then converted to mm/year using an annual operating duration of 340 days per year, derived from operational data obtained through direct interview.

$$\dot{t}_{\frac{mm}{year}} = \frac{E_R}{\rho_p} \times (3600 \times 24 \times 340) \times 10^3 \qquad (8)$$

The minimum allowable wall thickness (T_r) is determined in accordance with ASME B31.3 Process Piping standard, using the internal pressure design equation:

$$T_r = \frac{P \cdot D}{2(SE + PY)} + C \qquad (9)$$

where P= 1 MPa (design pressure), D= 89.1 mm (outer diameter), S= 110.32 MPa (allowable stress, ASME Table A-1), E= 0.85 (weld quality factor, ASME Table A-1B), Y= 0.4 (temperature correction factor, ASME Table 304.1.1), and C= 3 mm for corrosive environment (ASME B31.3, 2020; Revie & Uhlig, 2008). This yields a minimum design thickness of T_r= 3.47 mm. The remaining service life is then estimated as equation below, where t_0= 7.6 mm is the initial pipe wall thickness

$$L = \frac{t_0 - T_r}{\dot{t}_{mm/year}} \qquad (10)$$

3.4 Validation and Grid Independence

To ensure the reliability of the simulation results, the CFD-DPM model developed in this study was validated against the numerical results reported by Veiskarami and Saidi (2024), who conducted a comparable erosion simulation on a 90° elbow pipe under solid-gas flow conditions. The comparison between the present simulation results and the reference data shows a maximum relative error of 6.3%, which falls within an acceptable tolerance range for CFD-based erosion studies, as shown in Figure 4. This level of agreement confirms that the governing equations, turbulence model, and erosion model employed in this study can reproduce physically consistent erosion predictions.

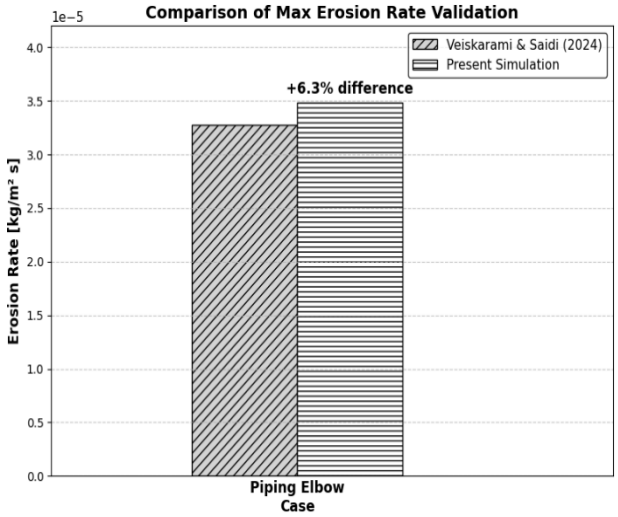

Figure 4: Validation Results

Grid independence testing was also carried out to ensure that the simulation results are not significantly influenced by the mesh density selected. Five levels of mesh refinement were tested, and the results were presented in Figure 5. The tests show that the solution stabilizes at the 20×20 division configuration (328,320 elements), beyond which further mesh refinement produces negligible change in the predicted maximum erosion rate. This configuration was therefore adopted for all subsequent simulation cases.

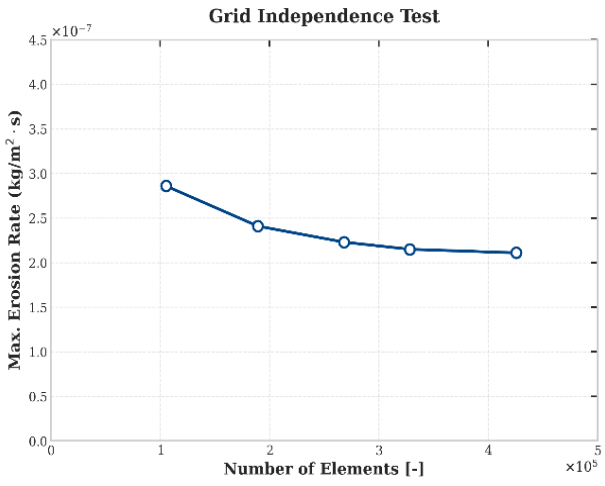

Figure 5: Grid Independence Test

International Current Journal of Engineering and Science (ICJES)
Volume 5, Issue 5, pp 9-17, May-2026
ISSN (Online): 2583-7257
Article DOI: https://doi.org/10.47001/ICJES/2026.505002

IV. RESULTS and DISCUSSION

4.1 Effect of Particle Size

The simulation results demonstrate that particle size has a dominant influence on erosion rate in the elbow pipe. As particle diameter increases from 150 µm to 350 µm, the maximum erosion rate rises substantially from 7.24 × 10^{-8} kg/m²s to 2.37 × 10^{-7} kg/m²s, an increase of approximately 227%. This behavior is physically intuitive: larger particles carry greater kinetic energy upon impact, and their higher inertia makes it increasingly difficult for the fluid to redirect their trajectory before they strike the outer wall of the elbow (Vahaji et.al., 2021). Figure 6 presents the relationship between particle diameter and maximum erosion rate, showing a consistently increasing trend as particle size grows from 150 µm to 350µm.

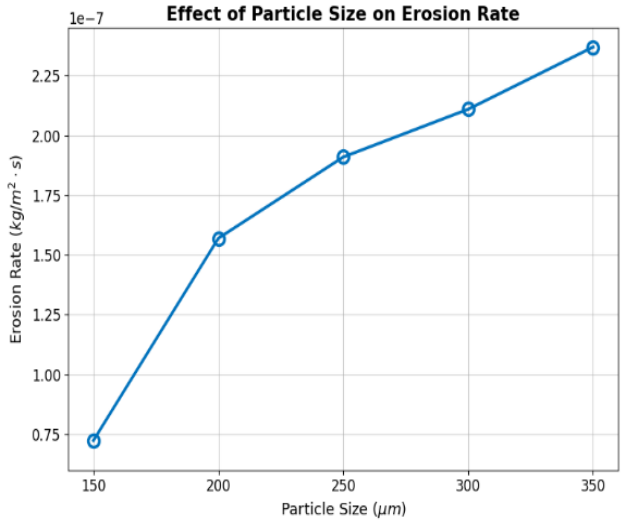

Figure 6: Maximum Erosion Rate for Varying Particle Diameters

4.2 Effect of Particle Concentration

Particle concentration proves to be the most influential parameter examined in this study. As concentration increases from 100 ppm to 300 ppm, the maximum erosion rate climbs from 1.36 × 10^{-7} kg/m²s to 4.09 × 10^{-7} kg/m²s, representing a threefold increase over the tested range. This is a direct consequence of the higher number of particles simultaneously present in the flow, more particles mean more frequent wall impacts per unit time, and the cumulative material loss accelerates proportionally. The near-linear relationship between concentration and erosion rate, as shown in Figure 7.

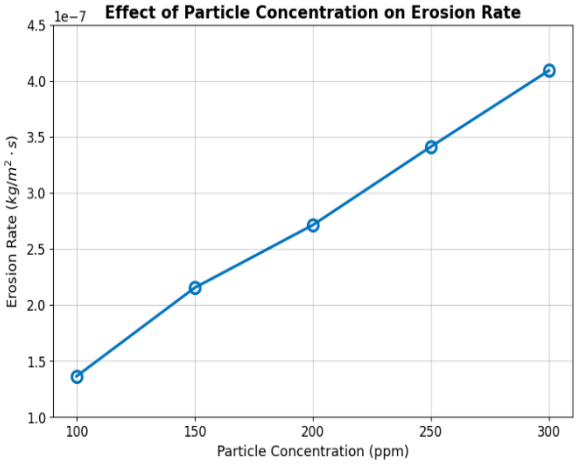

Figure 7: Maximum Erosion Rate for Varying Particle Concentrations

4.3 Effect of Flow Velocity

In contrast to particle size and concentration, flow velocity shows a comparatively moderate effect on erosion rate within the operational range investigated. As inlet velocity increases from 5.5 m/s to 7.4 m/s, the maximum erosion rate increases from 1.35 × 10^{-7} kg/m²s to 2.15 × 10^{-7} kg/m², a rise of approximately 59%. As shown in Figure 8, the trend is clearly positive and consistent with erosion theory, the higher velocity increases particle impact energy (Liu et.al., 2020). So that, the magnitude of change is notably smaller compared to the effects of particle size and concentration. This finding suggests that within the normal pump operating range of this system, velocity alone is not the primary erosion driver, and efforts to mitigate erosion should prioritize particle control over flow rate reduction.

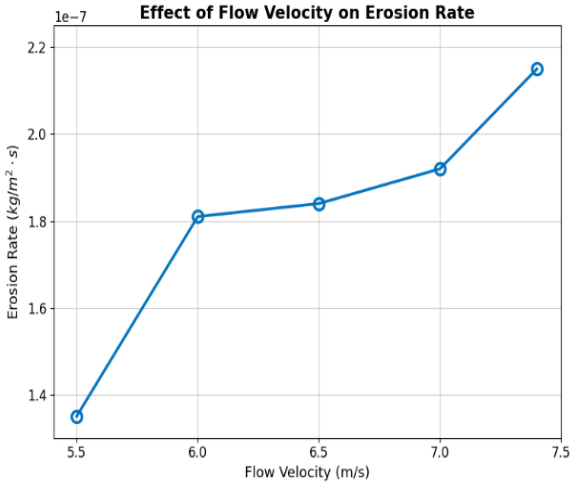

Figure 8: Maximum Erosion Rate for Varying Inlet Flow Velocities

International Current Journal of Engineering and Science (ICJES)
Volume 5, Issue 5, pp 9-17, May-2026
ISSN (Online): 2583-7257
Article DOI: https://doi.org/10.47001/ICJES/2026.505002

4.4 Effect of Elbow Geometry

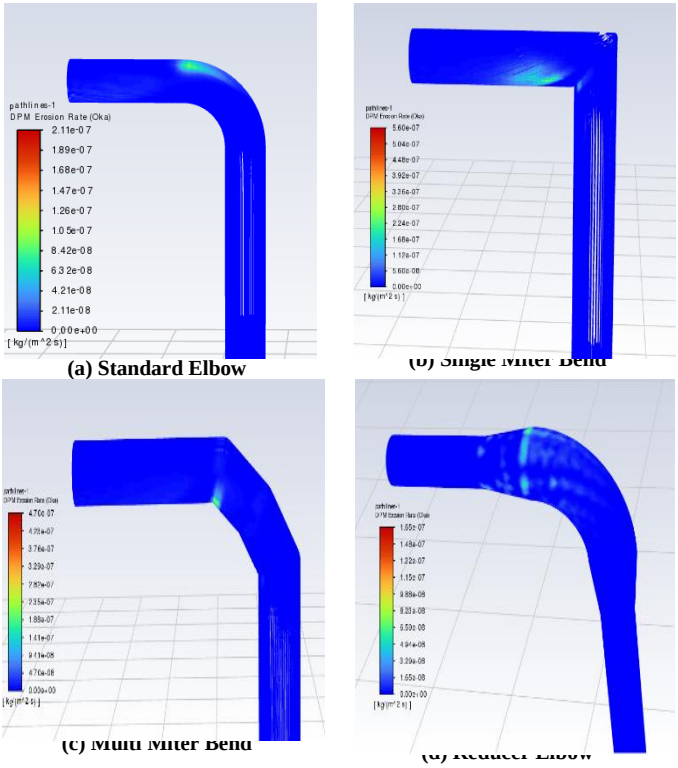

Figure 9: Erosion Rate Distribution Contours for Four Elbow Geometry Configurations

Figure 10 presents the erosion rate distribution contours for all four elbow geometry configurations obtained from the CFD-DPM simulation. The standard 90° elbow serves as the baseline with an erosion rate of 2.15 × 10^{-7} kg/m²s. Replacing it with a single miter bend results in a dramatic increase to 5.60 × 10^{-7} kg/m²s, more than 2.6 times the baseline. Due to the abrupt, right-angled deflection that concentrates particle impingement at a single sharp corner. The multi miter bend similarly produces an elevated erosion rate of 4.71 × 10^{-7} kg/m²s, though slightly lower than the single miter variant as the flow deflection is distributed across multiple smaller angular segments. The reducer elbow, on the other hand, achieves the lowest erosion rate among all variants at 1.65 × 10^{-7} kg/m²s, a 23% reduction relative to the standard elbow. As the gradual cross-sectional reduction redistributes flow momentum and reduces direct particle impingement intensity at the edge of the wall (Ma et.al., 2025). These results, as seen in Figure 10, collectively highlight that geometry optimization is a highly effective passive strategy for erosion mitigation that requires no modification to the operating conditions of the system.

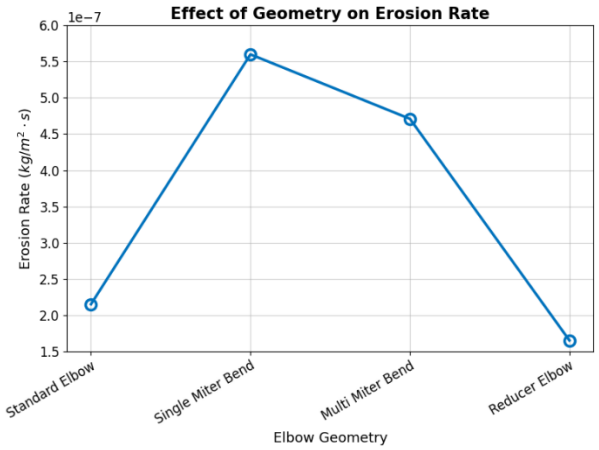

Figure 10: Maximum Erosion Rate for Varying Inlet Flow Velocities

4.5 Remaining Service Life (Wall Thinning)

Based on the wall thinning rates derived from the maximum erosion rate across all parametric variations, combined with the minimum allowable wall thickness of 3.47 mm calculated per ASME B31.3, the estimated remaining service life of the elbow pipe under each simulation condition is presented in Figures 11–14. The results reveal a wide range of predicted lifetimes — from a maximum of 15.3 years at the smallest particle diameter (150 µm) to as low as 1.65 years under the single miter bend geometry. Represent how sensitively the structural longevity of the pipe responds to changes in particle characteristics and elbow configuration. It is worth noting that these estimates represent an upper bound of the actual service life, as the erosion-corrosion synergy present in real seawater operating conditions would accelerate wall thinning beyond what the purely mechanical erosion model predicts.

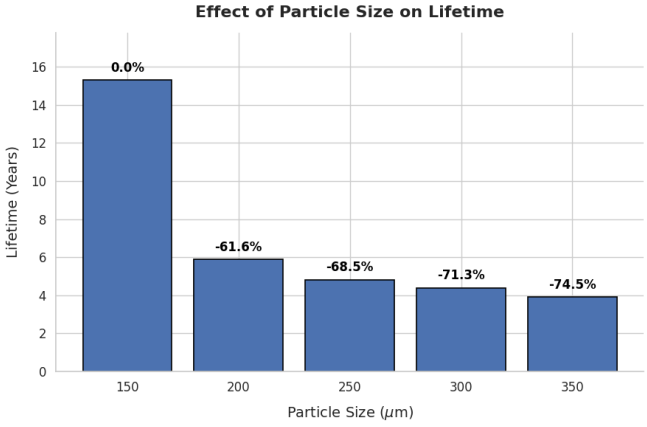

Figure 11: Estimated Remaining Service Life of Elbow Pipe under Varying Particle Diameters

International Current Journal of Engineering and Science (ICJES)
Volume 5, Issue 5, pp 9-17, May-2026
ISSN (Online): 2583-7257
Article DOI: https://doi.org/10.47001/ICJES/2026.505002

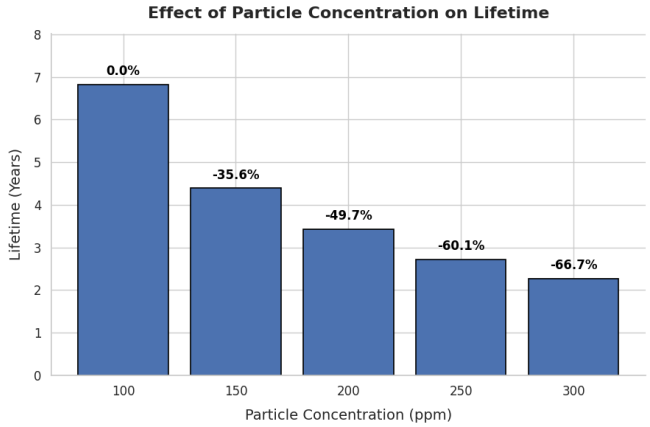

Figure 12: Estimated Remaining Service Life of Elbow Pipe under Varying Particle Concentrations

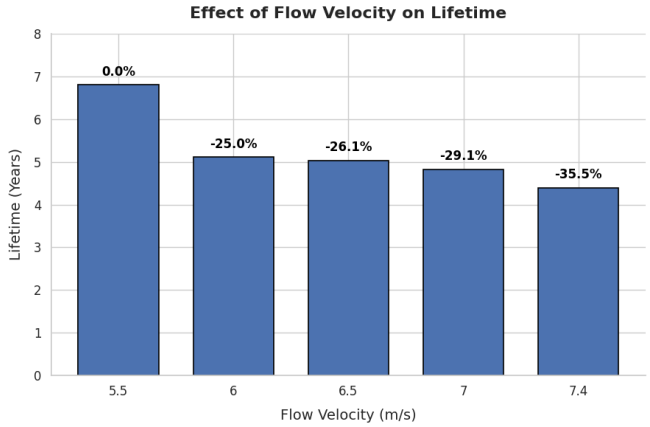

Figure 13: Estimated Remaining Service Life of Elbow Pipe under Varying Inlet Flow Velocities

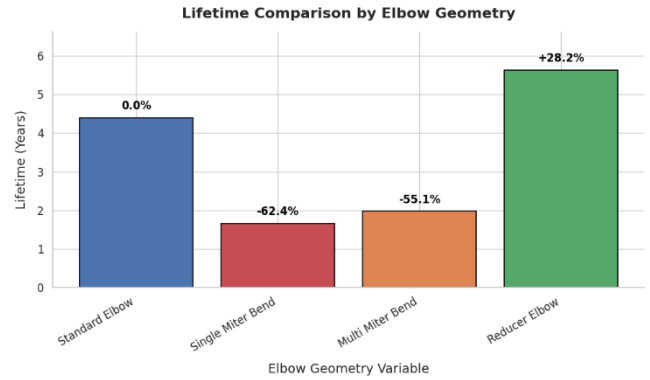

Figure 14: Estimated Remaining Service Life of Elbow Pipe across Elbow Geometry Configurations

V. CONCLUSION

Based on the analysis and calculations conducted in the previous chapter, the following results were drawn:

1. Among all parameters investigated, particle concentration proves to be the most influential factor governing erosion rate, followed by particle size and flow velocity. Increasing particle concentration from 100 to 300 ppm raises the maximum erosion rate threefold, from 1.36×10^{-7} to 4.09×10^{-7} kg/m²s, while increasing particle diameter from 150 to 350 µm produces a 227% rise in erosion rate from 7.24×10^{-8} to 2.37×10^{-7} kg/m²s. Flow velocity, by contrast, exerts a comparatively moderate influence within the operational range investigated. These findings suggest that controlling particle loading entering the system through improved filtration at the sea chest intake is the most effective operational strategy for mitigating erosion in marine seawater cooling piping..
2. Elbow geometry configuration has a decisive impact on erosion severity and should be considered a primary design variable in seawater piping systems. The single miter bend produces the most severe erosion at 5.60×10^{-7} kg/m²s with an estimated service life of only 1.65 years, while the reducer elbow achieves the lowest erosion rate of 1.65×10^{-7} kg/m²s and the longest estimated service life of 5.63 years — representing a 28.2% improvement over the standard 90° elbow baseline — making it the recommended geometry for erosion-critical seawater piping applications.
3. The remaining service life estimations based on ASME B31.3 minimum wall thickness criteria reveal that the structural longevity of the elbow pipe is highly sensitive to the combined effect of all investigated parameters. Under the most severe combination of conditions, the pipe reaches its minimum allowable wall thickness in under two years, underscoring the critical importance of periodic thickness monitoring and proactive maintenance scheduling for seawater supply piping in vessels operating in sediment-rich coastal and port environments.

REFERENCES

[1] Mahmoudi, O., & Shiri, Y. (2025). Impact of solid particle geometry, size, and intensity, coupled with fluid velocity, on erosion dynamics in elbow conduits. *Scientific Reports*, 15(1), 30880. https://doi.org/10.1038/s41598-025-16720-z.

[2] Yasser, E., Zhou, L., & El-Emam, M. A. (2025). CFD–DEM analysis of erosion in 90° elbow pipe induced by different particle shapes. *Powder Technology*, 466, 121453. https://doi.org/10.1016/j.powtec.2025.121453.

[3] Rahman, S., Khan, R., Niazi, U. M., Legutko, S., Khan, M. A., Ahmed, B. A., ... & Irfan, M. (2022). Performance prediction of erosive wear of steel for

International Current Journal of Engineering and Science (ICJES)
Volume 5, Issue 5, pp 9-17, May-2026
ISSN (Online): 2583-7257
Article DOI: https://doi.org/10.47001/ICJES/2026.505002

two-phase flow in an inverse U-bend. *Materials*, 15(16), 5558. https://doi.org/10.3390/ma15165558.

[4] Veiskarami, A., & Saidi, M. (2024). Numerical analysis of gas-solid flow erosion in different geometries as alternatives to a standard pipe elbow. *Powder Technology*, 448,120334. https://doi.org/10.1016/j.powtec.2024.120334

[5] Sridhar, K., Balasubramanian, V. (2022). Erosion–Corrosion-Resistant Coatings for Seawater Piping Components—A Review. In: KamachiMudali, U., Subba Rao, T., Ningshen, S., G. Pillai, R., P. George, R., Sridhar, T.M. (eds) A Treatise on Corrosion Science, Engineering and Technology. *Indian Institute of Metals Series. Springer, Singapore*. https://doi.org/10.1007/978-981-16-9302-1_30.

[6] Davidson, I., Cahill, P., Hinz, A., Kluza, D., Scianni, C., & Georgiades, E. (2021). A review of biofouling of ships' internal seawater systems. *Frontiers in Marine Science*. https://doi.org/10.3389/fmars.2021.761531.

[7] Martins, N. M. C., Carriço, N. J. G., Ramos, H. M., & Covas, D. I. C. (2014). Velocity-distribution in pressurized pipe flow using CFD: Accuracy and mesh analysis. *Computers & Fluids*, 105, 218–230. https://doi.org/10.1016/j.compfluid.2014.09.031

[8] Dou, X., Xiang, W., Li, B., Ju, M., Li, A., Zhang, D., & Li, Y. (2023). CFD-DPM modelling of solid particle erosion on weld reinforcement height in liquid-solid high shear flows. *Powder Technology*, 427, 118773. https://doi.org/10.1016/j.powtec.2023.118773.

[9] Mahmoudi, O., & Shiri, Y. (2025). Effects of the radii of curvature and the connecting length on erosion behavior in sequentially connected elbows. *Scientific Reports*, 15(1), 20874.https://doi.org/10.1038/s41598-025-04961-x.

[10] Y.I. Oka, K. Okamura, T. Yoshida, Practical estimation of erosion damage caused by solid particle impact: part 1: effects of impact parameters on a predictive equation, *Wear* 259 (1–6) (2005) 95–101, https://doi.org/10.1016/j.wear.2005.01.039.

[11] Y. Oka, T. Yoshida, Practical estimation of erosion damage caused by solid particle impact: part 2: mechanical properties of materials directly associated with erosion damage, *Wear* 259 (1–6) (2005) 102–109, https://doi.org/10.1016/j.wear.2005.01.040.

[12] ASME B31.3. (2020). Process Piping. *American Society of Mechanical Engineers*.

[13] Revie, R. W., & Uhlig, H. H. (2008). Corrosion and corrosion control: An introduction to corrosion science and engineering (4th ed.). *Wiley-Interscience*.

[14] Vahaji, S., Nguyen, N. H., Shang, Y., & Inthavong, K. (2021). Sedimentation effects on particle position and inertial deposition in 90° circular bends. *Powder Technology*, 393, 722-733.https://doi.org/10.1016/j.powtec.2021.07.072.

[15] Liu, Y., Chen, C., Wei, J., Liu, X., & Wang, X. (2020). Influence of abrasive hardness on erosion wear of abrasive air jets. *Journal of Central South University*, 27(2), 356–371. https://doi.org/10.1007/S11771-020-4301-6.

[16] Ma, J., Wen, F., Deng, Z., Wei, L., Ma, Y., Sun, H., ... & Li, X. (2025). Optimized design of a high-solid-content liquid elbow: an anti-erosion 3D twisted swirl plate structure. *RSC advances*, 15(27), 21934-21946. https://doi.org/10.1039/d5ra00012b.

Citation of this Article:

Muchammad, Budi Setiyana, & Galang Hardhian Prasetyo. (2026). CFD-DPM Based Prediction of Erosion Rate in Elbow Pipe under Seawater Flow Conditions. *International Current Journal of Engineering and Science (ICJES)*, 5(5), 9-17. Article DOI: https://doi.org/10.47001/ICJES/2026.505002

****

